A 24-31GHz 28nm FD-SOI CMOS 3:1 VSWR Resilient Inductive Hybrid Coupler-Based Doherty Power Amplifier

Gwennaël Diverrez[#1], Eric Kerhervé[#2], Magali De Matos[#3], Andreia Cathelin[$4]
[#]University of Bordeaux, IMS Laboratory, CNRS UMR 5218, Bordeaux INP, Talence, France
[$]STMicroelectronics, Crolles, France
{[1]gwennael.diverrez, [2]eric.kerherve, [3]magali.dematos}@ims-bordeaux.fr, [4]andreia.cathelin@st.com

***Abstract*— This paper presents a 28nm FD-SOI CMOS 24-31GHz broadband PA robust to 3:1 VSWR variations and exhibiting high linearity and efficiency up to deep power back-off. The circuit architecture proposes an energy efficient alternative to the Doherty PA enabling a continuous operation mode between symmetrical and asymmetrical modes. The PA exhibits 37% and 26% peak-6dB PBO PAE at 26GHz for asymmetrical/symmetrical operation, respectively. The measured results show compliance to the 5G NR and 64-QAM modulation schemes. The VSWR robustness is obtained thanks to the usage of hybrid couplers enabled in this topology. The PA core area occupies 0.90mm².**

***Keywords*— Doherty, inductive load, hybrid coupler-based, VSWR, continuously reconfigurable, CMOS 28nm FD-SOI.**

I. Introduction

The constant demand for multi-Gbits/s data rates has led to the development of the 5G new radio (NR) in the mm-wave bands. 5G relies on beamforming antenna arrays that require wideband mm-wave transmitters with moderate output power but high efficiency. However, these massive MIMO systems exhibit large impedance variations which induces VSWR variations, estimated at 3:1 for 5G. In addition, spectrally efficient modulation schemes (high-order QAM) over large bandwidths, resulting in high peak-to-average power ratio (PAPR), will be widely used to increase communications data rates. Therefore, broadband power amplifiers robust to 3:1 VSWR variations with linearity and efficiency up to deep power back-off (PBO) are of crucial interest for 5G.

Mm-wave dual drive core [1] and Class-F/F^{-1} [2] amplifiers exhibit linear and broadband behaviors with high PAE_{max} but limited efficiency with power back-off. In comparison, Outphasing [3] and Doherty [4] amplifiers provide high peak and deep back-off efficiency but are inherently narrowband and nonlinear. The LMBA [5] proposes a compromise between $PAE_{6dB\ PBO}$ boost and bandwidth although the load modulation control signal power consumption limits its overall efficiency. However, the performances of these solutions are very sensitive to VSWR variations. The hybrid coupler-based Doherty architecture [6] combines the efficiency enhancement of the Doherty PA with the VSWR resiliency of the balanced PA [7]. However, its robustness to VSWR variations is limited because no load is presented to dissipate output antenna mismatches.

To address these challenges, this paper proposes a multi-operation modes Doherty power amplifier, from a symmetrical mode with a $PAE_{6dB\ PBO}$ boost to a 2:1 asymmetrical mode with a $PAE_{9dB\ PBO}$ boost. The PA features a quadrature hybrid coupler-based architecture. Unlike the LMBA which uses a control signal to modulate the impedances presented at the two main amplifier outputs, the proposed solution uses a passive inductive load $L_{Doherty}$ to modulate the output load of its main amplifier. An adaptive biasing block is implemented with the peaking amplifier to optimize its power consumption at low power level and the overall linearity of the PA. A biasing fine tuning is enabled thanks to the 28nm FD-SOI body biasing extended feature. In section II, this paper describes the Doherty mode theory applied to the proposed PA architecture. The design of the PA is detailed in Section III. Section IV shows the measurements.

II. Inductive Coupler-Based Doherty Theory

A. From classical LMBA Theory to Innovative Doherty Theory

Fig. 1 presents a parallel between the conventional LMBA block diagram and the proposed architecture.

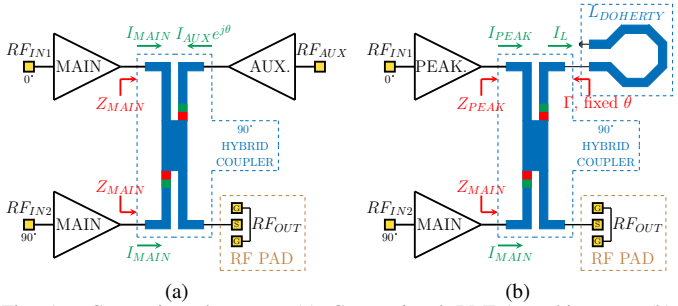

Fig. 1. Comparison between: (a) Conventional LMBA architecture; (b) Inductive hybrid coupler-based Doherty architecture.

In the case of an LMBA where a control signal is applied to the isolation port of its output hybrid coupler, the load impedance at the output of the main amplifier is :

$$Z_{MAIN_{(LMBA)}} = Z_0.(1 + \sqrt{2}\frac{I_{AUX}}{I_{MAIN}}e^{j\theta}) \quad (1)$$

where Z_0 is the reference impedance of the output coupler, I_{MAIN} the current of the main amplifier, I_{AUX} and θ the current and the phase of the injected signal, respectively.

Replacing the control signal with an inductive load and knowing that a reactive load reflects a signal with an attenuation ($|\Gamma|$) and a phase shift (θ), the load impedance at the output of the main amplifier becomes :

$$Z_{MAIN_{(DOHERTY)}} = Z_0.(1 + \sqrt{2}\frac{\Gamma.I_L}{I_{MAIN}}e^{j\theta}) \quad (2)$$

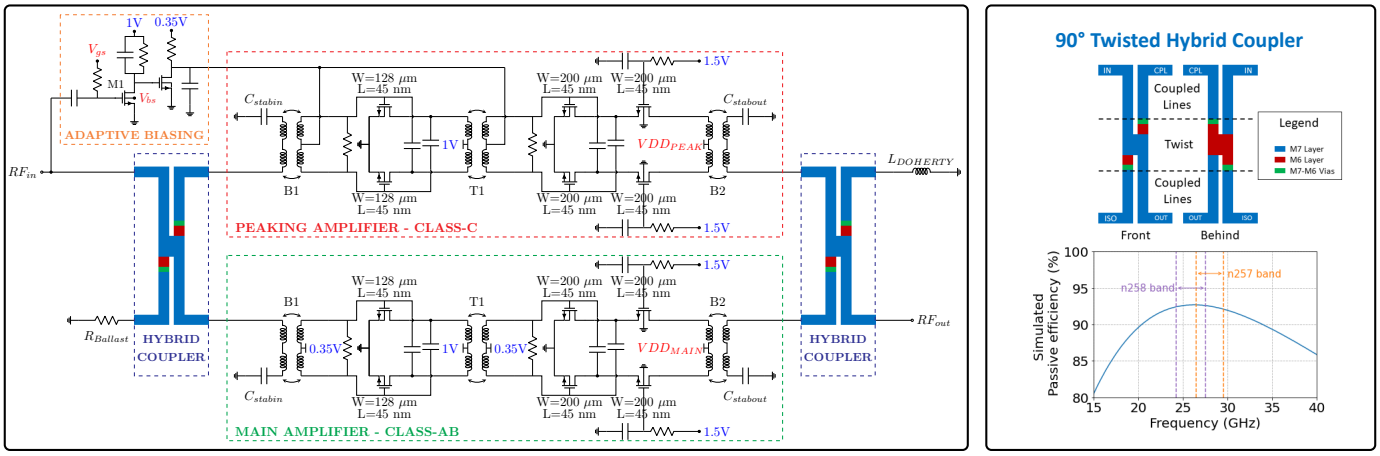

Fig. 2. Implemented inductive hybrid coupler-based Doherty power amplifier schematic.

B. The Peaking Amplifier is OFF (Low Power)

When the PA is operating at low power level, the peaking amplifier is turned off. As a result, half of the signal sent by the main amplifier is transmitted to the inductive load. Since the load is purely reactive, it reflects the signal with a phase shift induced by the load but without attenuation ($|\Gamma| = 1$) :

$$Z_{MAIN} = Z_0.(1 + e^{j\theta}) \tag{3}$$

Considering this statement, a load of $2Z_0$ is thus presented at the main amplifier output if $\theta = 2.k.\pi$ with k a natural number.

C. The Peaking Amplifier is ON (High Power)

When the Doherty power amplifier is operating at high power level, both amplifiers are on. The signals of the two amplifiers are sent to the inductive load in phase opposition. Therefore, no signal is transmitted to the inductive load and the impedance presented to the main amplifier is Z_0.

D. Broadband Behavior of the Inductive Load

The total phase shift θ considering the phase shift due to the hybrid coupler θ_{CPL} and the inductance θ_L is :

$$\theta = 2.\theta_{CPL} + \theta_L = -\frac{\pi}{2} + \theta_L \tag{4}$$

with $\theta_L = tan^{-1}\left(X_L/Z_0\right)$.

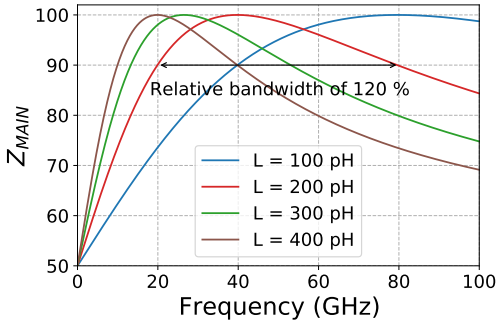

Fig. 3. Simulated Z_{MAIN} as a function of frequency.

As shown in Fig. 3, Z_{MAIN} exhibits a theoretical bandwidth of 120GHz. The choice of the impedance of the inductor is made to present an impedance close to 50 Ω.

III. Power Amplifier Design

The schematic of the inductive hybrid coupler-based Doherty PA is shown in Fig. 2. It consists of a main and a peaking amplifier with identical schematics, an adaptive biasing block, 90° hybrid couplers and an inductive load.

A. Elementary amplifier

Each amplifier consists of a common source driver followed by a cascode power cell and baluns/transformer for impedance matching and single to differential transformations. Capacitive neutralization using transistors is adopted to improve stability and gain. The output balun (B2) is designed to minimize its insertion loss (0.5dB) when the input balun (B1) and the intermatching transformer (T1) are designed to optimize the amplifier's gain bandwidth. The resistors placed between the gates of the common source transistors are used to flatten the gain of the amplifier. Stabilization capacitors are used on the ground port of baluns to improve their common mode rejection ratio (CMRR) and avoid amplitude imbalances.

B. Adaptive Biasing Block

An adaptive biasing block is implemented to allow the gradual transition of the peaking amplifier from an OFF-state at low power to an ON-state class-AB operation at high power. Thanks to this block, the auxiliary amplifier power consumption is optimized at low power level and the overall linearity of the Doherty PA is improved. Upon the biasing conditions of VDD_{MAIN} and VDD_{PEAK}, we identify two extremity operation modes: symmetrical and 2:1 asymmetrical. Indeed, a quarter reduction of the power supply reduces the output power of the amplifier by a factor of 0.56. Nevertheless, all other possible biasing conditions in between are possible.

C. 90° Hybrid Couplers

Twisted hybrid couplers (Fig. 2) are chosen for their wideband behavior and their low insertion losses to avoid PAE degradation [7]. Each coupler with its interconnects presents a wideband simulated passive efficiency of more than 85% in the 17-40GHz band with a maximum of 93% at 27GHz. The output hybrid coupler enables the overall VSWR resiliency.

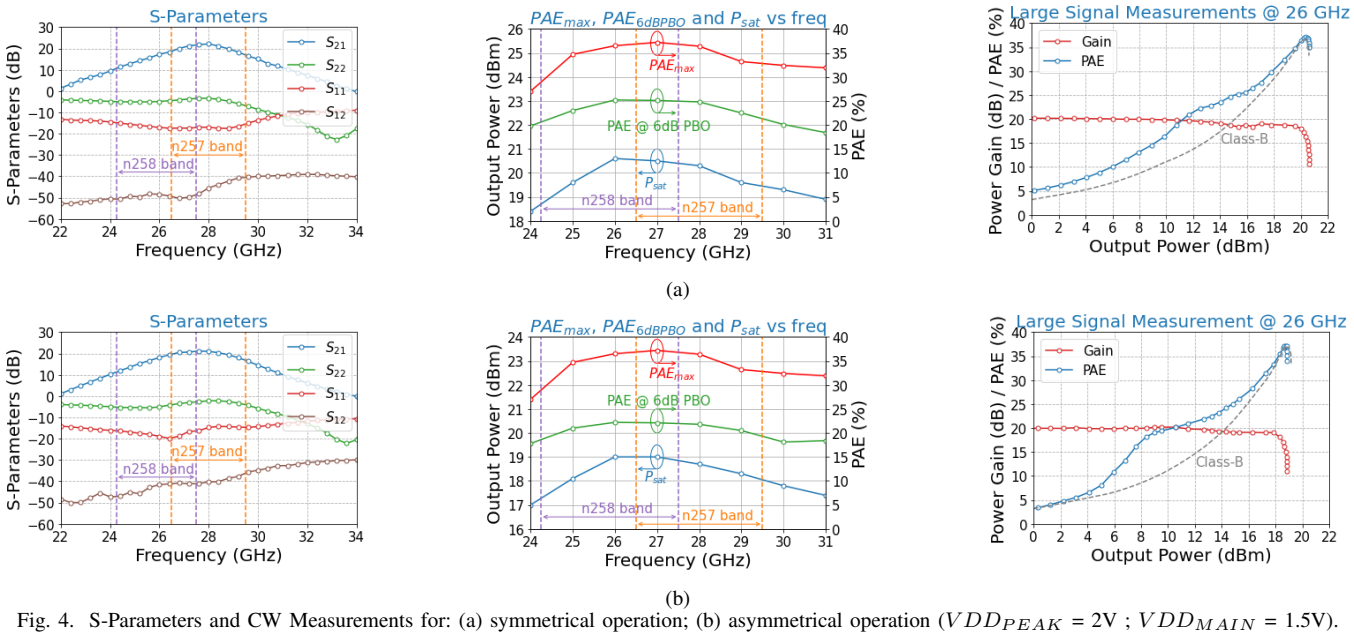

Fig. 4. S-Parameters and CW Measurements for: (a) symmetrical operation; (b) asymmetrical operation (VDD_{PEAK} = 2V ; VDD_{MAIN} = 1.5V).

IV. Measurement Results

The proposed PA (Fig. 5) is implemented in a 28nm FD-SOI CMOS 8ML process with a core area of 0.90mm².

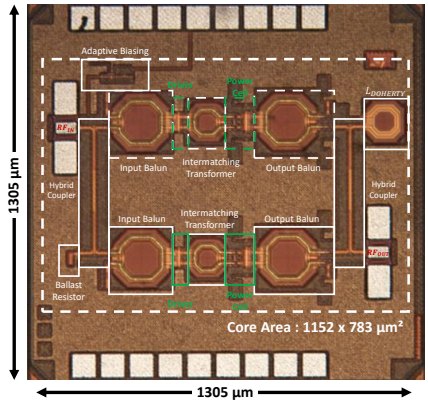

Fig. 5. Die micrograph of the proposed 28nm FD-SOI CMOS PA.

A. S-Parameters

Small-signal measurements (Fig. 3) show a maximum gain of 20.5dB for both operating modes at 28GHz. Thanks to the coupler-based structure, the input is well matched from 22 to 34GHz (S_{11} < -10dB) and covers n257 and n258 bands.

B. CW Measurements

Concerning the PA large-signal measurements at 26GHz, the symmetrical mode Doherty PA achieves a high PAE_{max} and a PAE_{6dBPBO} enhancement (37% / 26%). On the other hand, the asymmetrical mode PA exhibits a PAE_{9dBPBO} boost (20%) thanks to its 2:1 asymmetry. Over a frequency range of 24.25 to 30GHz (n257 and n258 bands), both operation modes of the Doherty PA demonstrate wideband behavior with >30% PAE_{max} and > 19% PAE_{6dBPBO}.

C. VSWR Measurements

Fig. 6 and Fig. 7 show the large-signal 3:1 VSWR measurements at 26 and 29GHz for the proposed symmetrical Doherty power amplifier compared to those of the main amplifier in standalone implementation, as a reference point. Each angle point is separated from the next by 30°.

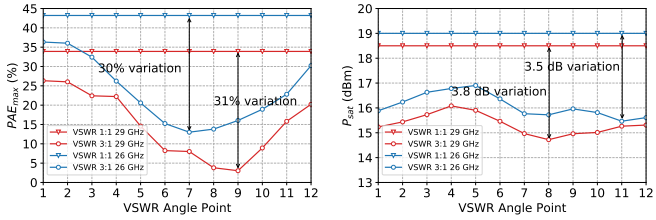

Fig. 6. VSWR Measurements of the main amplifier: (a) PAE_{max}; (b) P_{sat}.

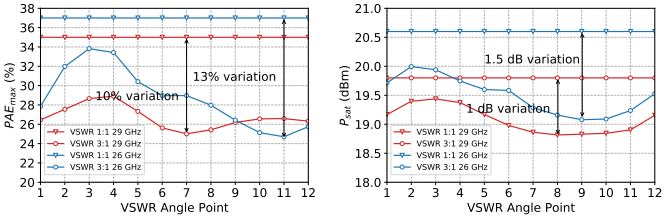

Fig. 7. VSWR Measurements of the Doherty PA: (a) PAE_{max}; (b) P_{sat}.

The first observation is that there is no circuit destruction after 1 hour of operation under every 5:1 VSWR conditions. Moreover, we can state that the proposed solution enables a minimal degradation of performances at VSWR 3:1: only 1.5/1dB variation for the full version vs 3.8/3.5dB for the unprotected solution, for P_{sat} at 26/29 GHz. This observation is also confirmed for PAE_{max} with a variation of only 13/10% for the full version vs 31/30% for the unprotected solution.

Table 1. Comparison with the state of the art of mm-wave PAs for the 5G NR FR2 bands.

Reference	This Work		[1] ISSCC'21	[2] ISSCC'18	[3] ISSCC'20	[4] ISSCC'22	[5] ISSCC'21	[6] ISSCC'20
Technology	28nm FD-SOI		45nm RF-SOI	130nm SiGe	45nm RF-SOI	55nm bulk	28nm CMOS	45nm RF-SOI
Architecture	Symmetrical Doherty	Asymmetrical Doherty	Dual-Drive PA Core	Continuous Class-F/F^{-1}	Inverse Outphasing	3-way Doherty	Doherty-Like LMBA	Doherty Ser./Par.
Supply (V)	2.0 (Main) 2.0 (Aux)	1.5 (Main) 2.0 (Aux)	1.9	1.9	2.0	2.4	1.5	2.0
Frequency (GHz)	26.0	26.0	28.0	28.5	29.0	28.0	39.0	39.0
Gain (dB)	19	20	18.0	18.2	13.2	30.0	32.6	20
P_{sat}(dBm)	20.5	20.5	20.4	20.0	30.0	16.1	18.0	12.5
PAE_{max} (%)	37	37	48.3	43.5	41.3	25.2	32	33.3
$PAE_{6dB\ PBO}$(%)	25	22	23*	19*	30.6	20.4	24.2	22.4
$PAE_{12dB\ PBO}$(%)	13.5	14.2	6*	6*	10	14.2	8*	10*
PAE_{max}@7GHz (%)	31	31	N.A.	27*	17*	N.A.	30*	N.A.
VSWR Immunity	3:1 VSWR	3:1 VSWR	No	No	No	No	No	3:1 VSWR
Modulation scheme	64-QAM	64-QAM	64-QAM	64-QAM	64-QAM	64-QAM	64-QAM	64-QAM
PAPR (dB)	6.7	6.7	9.6*	6	6	6	6	6
Data Rate (Gbits/s)	1.5	1.5	6	6	3	1.5	12	3
EVM_{rms}(dB)	-27.3	-26.6	-25.0	-27.6	-25.3	-25.2	-25.0	-22.7
P_{avg}(dBm)	13.1	10.4	10.7	10.7	16.0	17.7	16.0	12.2
PAE_{avg}(%)	23.0	20.0	15.5	21.4	23.8	17.5	22.0	16.1
ACLR (dBc)	-25.9	-25.2	-26.6	N.A.	-33	-27*	-25*	-25.4
Core Area (mm^2)	0.90	0.90	0.21	0.29	0.96	0.54	1.44+	1.18

\# graphically estimated + Chip area N.A.: Not Available $\mathrm{PAE_{max@7GHz}}$: minimum $\mathrm{PAE_{max}}$ over a 7GHz band around the PA's $\mathrm{PAE_{max}}$

D. Modulated signals Measurements

Fig. 8 shows modulation tests of the Doherty PA in both extreme operation modes using single-carrier 64-QAM signals without DPD at 26GHz. For a 1.5Gb/s 64-QAM signal, the EVM is below -27.3dB with an average output power P_{avg} of 13.1dBm and a PAE_{avg} of 23% for the symmetrical operation mode. Similar measurements were done for the asymmetrical amplifier where the PA achieves a P_{avg} of 10.4dBm and a PAE_{avg} of 20% with an EVM_{rms} of -26.6dB. Hence, the Doherty PA demonstrates linearity performance consistent with the 5G standard specifications for both modes.

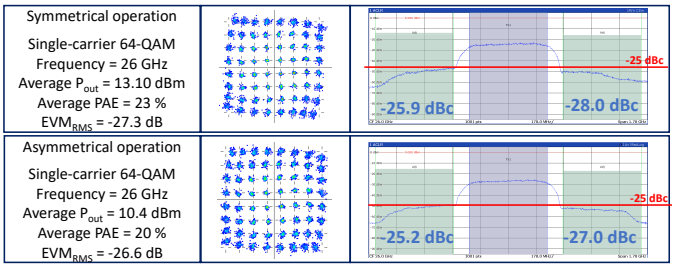

Fig. 8. Measured constellation diagram and spectrum at 26GHz.

V. Conclusion

Table 1 presents the full set of measured results for the presented PA in its two extreme operation modes, and a comparison with the state of the art. For simplicity, the two configurations shown in the table refer to extreme operating modes of the PA (2:1 and 1:1 Aux/Main ratios). Nevertheless, a continuity of operation modes exists between these two modes. To our knowledge, the circuit demonstrates the highest peak/back-off PAE among mm-wave silicon PAs with VSWR variations robustness, thanks to its passive inductive load for both operation modes. In addition, this architecture contains one amplifier less than the LMBA architecture, which reduces its complexity and silicon footprint for better efficiency performances. Thanks to its asymmetrical 2-way architecture that avoids recombination losses, the PA achieves the best PAE_{max} and PAE_{6dBPBO} among asymmetrical Doherty PAs. The PA also features a wideband Doherty architecture over a 7GHz band thanks to the wideband hybrid couplers replacing the conventional Doherty PAs quarter-wave line impedance inverter. This architecture's efficiency enhancement technique with PBO enables better efficiency performances with 5G modulated signals (high PAPR) than previous work. 5G NR FR2 PA measurements demonstrate state-of-the-art linearity performances for Doherty architectures. In summary, the presented architecture is able to achieve high peak and deep power back-off PAE with a 3:1 VSWR immunity while maintaining linearity, making it suitable for 5G NR FR2 wireless communication links.

Acknowledgment

The authors would like to thank STMicroelectronics for chip fabrication and Rohde & Schwarz for measurements.

References

[1] E. Garay *et al.*, "26.3 A mm-Wave Power Amplifier for 5G Communication Using a Dual-Drive Topology Exhibiting a Maximum PAE of 50% and Maximum DE of 60% at 30GHz," ISSCC, 2021.

[2] T.-W. Li *et al.*, "A continuous-mode harmonically tuned 19-to-29.5GHz ultra-linear PA supporting 18Gb/s at 18.4% modulation PAE and 43.5% peak PAE," ISSCC, 2018.

[3] S. Li *et al.*, "A 28GHz Current-Mode Inverse-Outphasing Transmitter Achieving 40%/31% PA Efficiency at Psat/6dB PBO and Supporting 15Gbit/s 64-QAM for 5G Communication," ISSCC, 2020.

[4] Z. Ma *et al.*, "A 28GHz Compact 3-Way Transformer-Based Parallel-Series Doherty Power Amplifier With 20.4%/14.2% PAE at 6-/12-dB Power Back-off and 25.5dBm PSAT in 55nm Bulk CMOS," ISSCC, 2022.

[5] V. Qunaj and P. Reynaert, "A Doherty-Like Load-Modulated Balanced Power Amplifier Achieving 15.5dBm Average Pout and 20% Average PAE at a Data Rate of 18Gb/s in 28nm CMOS," ISSCC, 2021.

[6] N. S. Mannem *et al.*, "A Reconfigurable Series/Parallel Quadrature Coupler Based Doherty PA in CMOS SOI with VSWR Resilient Linearity and Back-Off PAE for 5G MIMO Arrays," ISSCC, 2020.

[7] G. Diverrez *et al.*, "A 24-31GHz 28nm FD-SOI CMOS Balanced Power Amplifier Robust to 3:1 VSWR for 5G Application," EuMC, 2022.